14 Sep 1992

Diffraction In The Binary Encounter Electron Peak Observed In Collisions Of 0.6 MeV Amu⁻¹ I7+, I23+ And Au11+ Projectiles With He And Ar

W. Wolff

J. L. Shinpaugh

H. E. Wolff

Ronald E. Olson
Missouri University of Science and Technology, olson@mst.edu

et. al. For a complete list of authors, see https://scholarsmine.mst.edu/phys_facwork/2593

Recommended Citation

W. Wolff et al., "Diffraction In The Binary Encounter Electron Peak Observed In Collisions Of 0.6 MeV Amu⁻¹ I7+, I23+ And Au11+ Projectiles With He And Ar," *Journal of Physics B: Atomic, Molecular and Optical Physics*, vol. 25, no. 17, pp. 3683 - 3691, IOP Publishing, Sep 1992.
The definitive version is available at https://doi.org/10.1088/0953-4075/25/17/019

Journal of Physics B: Atomic, Molecular and Optical Physics

Diffraction in the binary encounter electron peak observed in collisions of 0.6 MeV amu^{-1} I^{7+} I^{23+} and Au^{11+} projectiles with He and Ar

To cite this article: W Wolff *et al* 1992 *J. Phys. B: At. Mol. Opt. Phys.* **25** 3683

View the article online for updates and enhancements.

J. Phys. B: At. Mol. Opt. Phys. 25 (1992) 3683–3691. Printed in the UK

Diffraction in the binary encounter electron peak observed in collisions of 0.6 MeV amu^{-1} I^{7+}, I^{23+} and Au^{11+} projectiles with He and Ar

W Wolff†‡, J L Shinpaugh†, H E Wolff†‡, R E Olson§, J Wang§, S Lencinas†, D Piscevic†, R Herrmann† and H Schmidt-Böcking†

† Institut für Kernphysik, Universität Frankfurt, Frankfurt am Main, Federal Republic of Germany

‡ Instituto de Física, Universidade Federal do Rio de Janeiro, Rio de Janeiro, Brazil

§ University of Missouri at Rolla, Rolla, MI, USA

Received 6 April 1992, in final form 26 May 1992

Abstract. Relative double differential cross sections for electron emission from collisions of 0.6 MeV amu^{-1} I^{7+} and I^{23+} projectiles with Ar and Au^{11+} projectiles with He were measured for electron energies from 100 eV to 2000 eV and for angles from 0° to 50°. Experimentally observed sudden shifts of the position of the binary encounter peak were interpreted as resulting from quantum interference in the scattering of target electrons from the partially stripped projectile ion. To this end calculations for the elastic scattering of free electrons initially at rest in the laboratory reference frame from the screened projectile field as well as model calculations of binary encounter electron production taking into account the target Compton profile were performed and compared with the experimental results. Good agreement was obtained for the angular locations of these shifts as well as for the angular distribution of the binary encounter electron yield.

1. Introduction

The binary encounter peak is a distinct feature of energy spectra of electrons ejected during collisions of charged projectiles with atoms (Stolterfoht *et al* 1974). It originates from hard collisions and consequently leads to large energy transfer between target electrons and projectile. The binary peak can be treated, to a good approximation, as the elastic scattering of a target electron in the field of the projectile without taking into account the presence of the residual target atom. In this simple picture an electron originally at rest in the laboratory reference frame is expected to acquire through the scattering process a velocity $v_e^L = 2V_p \cos\vartheta^L$, where V_p is the projectile velocity and ϑ^L the angle of observation. The basic validity of this picture was demonstrated by Lee *et al* (1990) for bare projectiles up to F^{9+} at zero degree observation angle. In particular it was verified by these authors that the binary encounter cross sections scaled with the square of the bare projectile charge Z_p, as would be expected from the Rutherford formula for the elastic scattering of free electrons in the field of a point charge Z_p. The position and shape of the binary encounter peak were reproduced within the impulse approximation (IA) by taking into account the binding energy of the target electrons and the target Compton profile.

Different and unexpected results, initially referred to as 'anomalies', were obtained for the production of binary encounter electrons in collisions involving 'clothed' ions.

An experimental investigation of the binary encounter electron yield at zero degree observation angle for 1–2 MeV amu^{-1} fluorine ions of various charge states by Richard *et al* (1990) revealed that this yield decreased rather than increased with increasing ionic charge, i.e. fluorine ions of lower charge produced more binary encounter electrons than higher charged ions. At non-zero degree observation angles a 'dip' superposed on the binary encounter peak was reported for 1.4 MeV amu^{-1} $U^{32+,33+}$ projectiles incident on rare gases by Kelbch *et al* (1989). Subsequently it was realized that both phenomena are related, and an explanation of the 'anomalies' encountered in binary encounter electron production in terms of a quantum interference effect was put forward in a series of papers by Reinhold *et al* (1990, 1991), Olson *et al* (1990), Shingal *et al* (1990), Bhalla and Shingal (1991), Jagutzki *et al* (1991) and Schultz and Olson (1991). Basically the BE electron is no longer scattered in a pure Coulomb field, but in a potential statically screened by the projectile electrons. The screening gives rise to marked deviations from the Rutherford cross section, and, depending on the degree of screening and the velocity of the electron, strong diffraction effects may result. The phenomenon was observed experimentally by Kessler and Lindner (1965) in the elastic scattering of electrons with energies ranging from 200 eV up to 4 keV by a Hg target. Since BE electrons are target electrons scattered elastically in the field of the projectile, similar diffraction effects are expected for clothed projectiles.

Strong experimental evidence for such a connection has been presented in investigations with 1.0 MeV amu^{-1} U^{21+} (Reinhold *et al* 1991) and 0.6 MeV amu^{-1} Au^{11+} projectiles (Hagmann *et al* 1992). In the first case a central depression was observed in the binary encounter peak at the observation angle of 35°. An accompanying calculation for the elastic scattering of electrons initially at rest in the laboratory frame by U^{21+} revealed a deep diffraction minimum in the cross section at a laboratory angle of 37.5°. In the Au^{11+} case a very pronounced splitting of the binary encounter peak observed around 30° might be similarly caused by a minimum in the elastic scattering cross section for electrons by Au^{11+} at an angle of 32.5°.

For both U^{21+} and Au^{11+} a second deep diffraction minimum exists in the calculated elastic scattering cross sections at more forward laboratory angles. Reinhold *et al* (1991) carried out a model calculation for sufficiently small angles to find that for the U^{21+} system this second minimum did not reflect itself as an additional 'anomaly' in the binary encounter peak. This result, however, was considered by these authors to be sensitive to the detailed form of the model potential used for U^{21+}. On the other hand the influence of this second diffraction minimum upon the binary encounter peak has still to be established experimentally, since the experiments did not cover small enough angles of observation.

Since the small angle behaviour of the binary encounter peak is not known, the present investigation was undertaken in order to extend BE cross section measurements to extreme forward angles. Furthermore diffraction effects have been established so far only for a few very heavy projectiles (Au^{11+}, $U^{21+,32+,33+}$), so it is important that additional research including lighter projectiles should be performed.

2. Experimental arrangement

The experiments were carried out at the Emperor tandem accelerator of the Max-Planck-Institut für Kernphysik, Heidelberg. Well collimated ion beams traversed a gas cell, whose pressure was kept within the single collision regime. Electron spectra were taken with an electrostatic 127° cylinder spectrometer equipped with a channeltron and modified so as to allow measurements down to a zero degree observation angle. Angular and energy resolution of the spectrometer were ±1° and 5% respectively. The voltage applied to the spectrometer plates was advanced in constant steps corresponding to equal amounts of accumulated beam charge, so the spectra are independent of fluctuations in the beam current. For mechanical reasons the maximum angle for this spectrometer was limited to 35°, so a double-focusing hemispherical spectrometer having the same angular and energy resolution was employed for angles from 35° to 50°. Detailed descriptions of the experimental arrangement are given by Kelbch (1991) and Kelbch *et al* (1992).

3. Results and discussion

Relative double differential cross sections $d^2\sigma/dE\,d\Omega$ for electron production from 0.6 MeV amu^{-1} I^{23+} and I^{7+} projectiles incident on Ar and from Au^{11+} projectiles incident on He are given in figures 1 and 2 for observation angles ϑ^L from 0° to 35°. Cross sections obtained with the hemispherical spectrometer for angles from 35° to 50° for I^{7+} incident on Ar are shown separately in figure 3, which also includes calculated model cross sections discussed below. The same relative units are used for the three collision systems, so cross sections for different projectiles and targets can be compared directly.

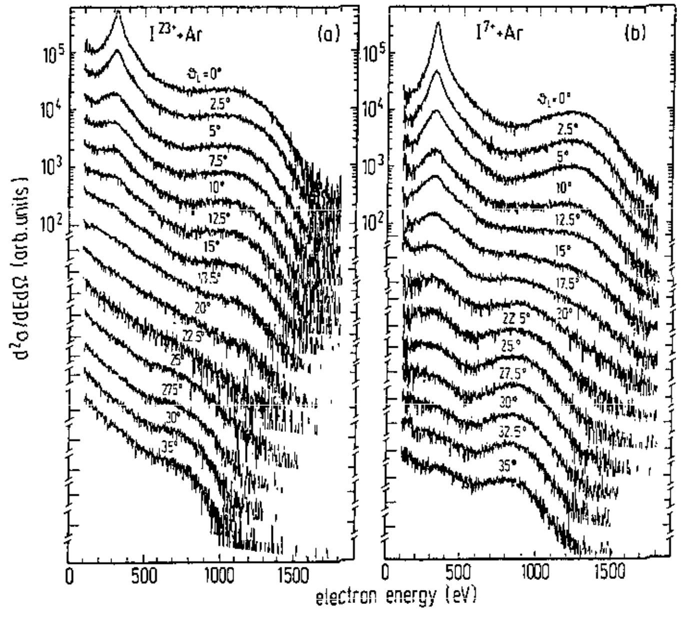

Figure 1. Relative double differential cross sections $d^2\sigma/dE\,d\Omega$ (in arbitrary units) for electron production by the collision of 0.6 MeV amu^{-1} I^{23+} (*a*) and I^{7+} (*b*) projectiles with argon. The logarithmic scale indicated applies to the 0° cross sections. The same scale, but shifted downwards, applies for the other angles. The base line from which the respective logarithmic scale starts is indicated for each angle.

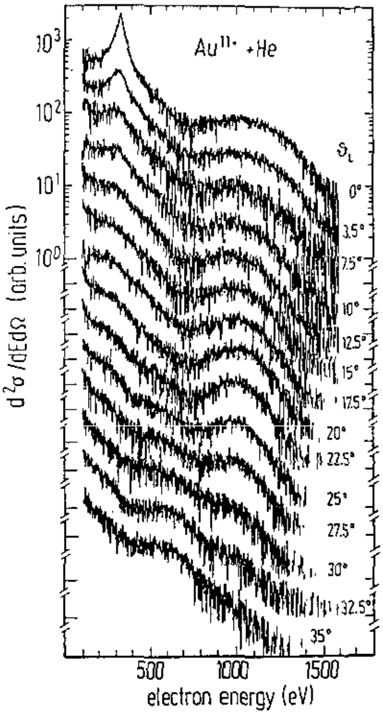

Figure 2. Relative double differential cross sections for electron emission from 0.6 MeV amu^{-1} Au^{11+} projectiles incident on helium.

At small ϑ^L the cross sections are dominated by two features, a low energy $v_e^L = V_p$ peak with its characteristic cusp shape at 0° due to the processes of electron capture to the continuum (ECC) and electron loss to the continuum (ELC) (Salin 1969, Macek 1970, Drepper and Briggs 1976), and a single binary encounter peak broadened by the target Compton profile. With increasing angle the intensity of the peak starts to decrease, but its centre position stays fixed, i.e. does not follow the well known $\cos^2 \vartheta^L$ law expected from simple kinematic considerations. At an angle specific to the projectile–target combination, the binary encounter intensity begins to shift to a new position of lower energy a few hundred eV apart from the original position occupied at very forward angles. In the case of I^{7+} and I^{23+} this shift is completed within a rather narrow angular interval. In the case of Au^{11+} this interval is broader and the two positions are more separated, making the binary peak appear to split into two components which coexist over a broad angular interval. At larger angles the binary encounter strength is confined to the new location of lower energy, which again does not show any $\cos^2 \vartheta^L$ dependence.

The present results for Au^{11+} (figure 2) represent an extension of the data of Hagmann *et al* (1992) to smaller angles. Cross sections for the elastic scattering of target electrons at rest in the laboratory reference frame (and hence possessing an energy of 327 eV in the projectile frame) off the three projectiles used in this work were calculated from model potentials by the method outlined in Schultz and Olson (1991) and are given in figure 4(*a*). Cross sections and scattering angles refer to the laboratory reference frame. As already mentioned the deep diffraction minimum in the electron elastic scattering cross section for Au^{11+} at a laboratory angle of 32° is

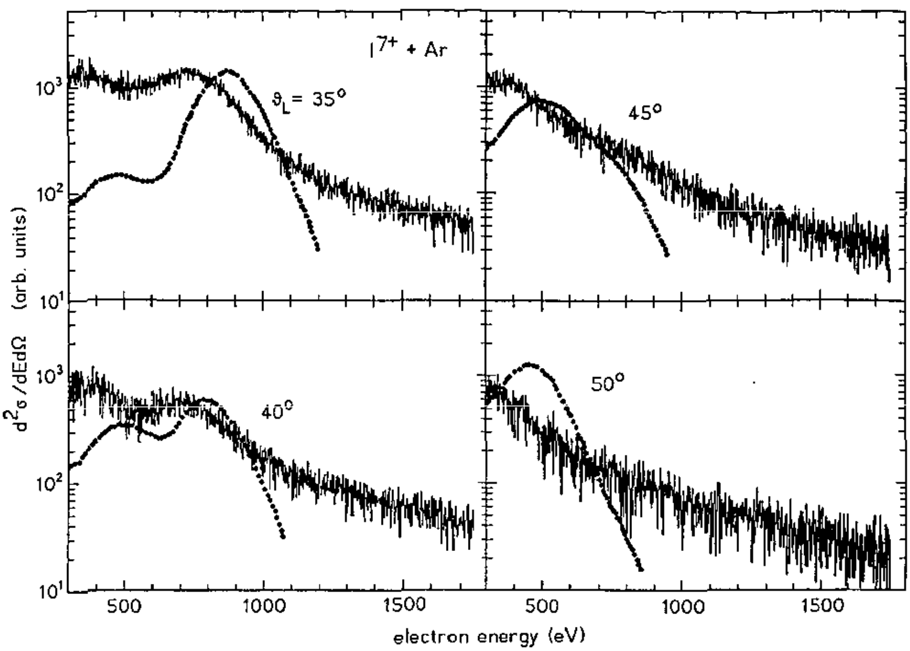

Figure 3. Relative DDCS, expressed in the same relative units as figures 1 and 2, for electron emission from 0.6 MeV amu^{-1} I^{7+} projectiles incident on Ar for observation angles from 35° and 50°. These data were taken with a hemispherical double-focusing spectrometer. The dotted curves represent the result of a model calculation explained in the text, and are arbitrarily normalized.

very probably responsible for the pronounced splitting of the BE feature observed at angles around 30°. The second deep diffraction minimum at 12° laboratory angle, however, does not manifest itself as a discernible variation in shape or strength of the binary encounter peak, as becomes clear upon inspection of the small angle cross sections of figure 2. Rather the peak becomes progressively broader and stronger as 0° is approached.

The experimental cross sections for electron production from collisions of I^{23+} with Ar (figure 1(*a*)) show a binary encounter peak which behaves very differently from the Au^{11+} case. For angles up to 17.5°, the peak is centred at 1100 eV and its intensity decreases rapidly with increasing angle. At 20° and 22.5° there is so little BE strength left that the electron production cross sections are almost featureless exponentials. A tiny residue of the original BE peak at 1100 eV is still discernible at 20°, while a similarly weak shoulder begins to appear at 22.5° at the new position of 750 eV. This shoulder then develops into the BE peak at larger angles, so the BE strength is found to shift between two discrete positions. A diffraction minimum present in the calculated elastic scattering cross section of 327 eV electrons by I^{23+} at 24° is in all probability responsible for the disappearance of binary encounter strength at 20° and 22.5°.

The electron production cross sections for I^{7+} incident on Ar (figures 1(*b*) and 3) exhibit an angular distribution pattern different from both the Au^{11+} and I^{23+} cases. For small angles up to 12.5° the binary encounter strength is located at 1250 eV and for angles above 20° at 750 eV. Around 15° the binary encounter intensity shifts from the higher to the lower position, giving rise, at that angle, to a very broad BE distribution

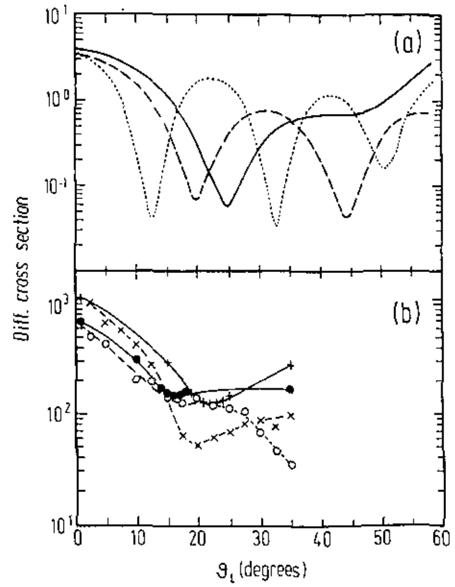

Figure 4. (*a*) Model cross sections $d\sigma/d\Omega$ (in atomic units) for the elastic scattering of 327 eV electrons by I^{23+} (full curve), I^{7+} (broken curve) and Au^{11+} (dotted curve) calculated by the method outlined in Schultz and Olson (1991). Cross sections and scattering angles refer to the laboratory reference frame, where the electrons are initially at rest. (*b*) Experimental and calculated binary encounter electron yields $d\sigma/d\Omega$ for the collision systems I^{7+} and I^{23+} on argon. The connecting lines are to guide the eye only. Full curves connect calculated yield points, while broken curves connect data points. See text for normalization of experimental data points. ○, exp, I^{7+}; ×, exp, I^{23+}; ●, calc, I^{7+}; +, calc, I^{23+}.

with a slight central depression. The calculated cross section for the elastic scattering of 327 eV electrons by I^{7+} exhibits a diffraction minimum at a laboratory angle of 19°, which is probably responsible for this shift. The effect of a second deep diffraction minimum, located at 45°, upon the BE peak escapes experimental verification, however. While there is still some binary intensity visible at 40° in figure 3, it has almost vanished at 45° and no trace of it is left at 50°.

Up to this point the observed sudden changes in position of the BE peak have been related to diffraction minima in the elastic scattering cross sections for electrons with a single fixed projectile frame energy (327 eV). Since the diffraction patterns are velocity dependent, a more realistic calculation, capable of reproducing the shape of the binary encounter peak, must take into account the initial velocity distribution of the scattered electrons determined by the target Compton profile. This is done in an impulse approximation adapted from the one used ealier for electron loss (Wang *et al* 1991). Briefly, in the projectile rest frame, the ionization cross section is given by convoluting over momenta the product of the elastic scattering cross section and the Compton profile. It should be noted that kinematics and energy conservation allow only a restricted subset of momenta contributing to a given final state. The cross section for elastic scattering is calculated by partial wave expansions (up to $l=40$) in the field of the projectile. The resulting ionization cross section after the convolution is transformed into the target rest frame. For many-electron targets like Ar, only the outermost shell electrons are included. The electrons are assumed to be independent of each other.

Initially each electron is described by a single zeta wavefunction, where zeta is the effective charge derived from the ionization potential.

The double differential model cross sections calculated in this way for I^{7+} and I^{23+} incident on argon are shown in figure 5 for selected angles of observation between 1° and 35°. The results obtained for I^{7+} for angles from 35° to 50° are included in figure 3. These model cross sections can be compared directly to the corresponding experimental cross sections. The marked structures in the calculated binary encounter peak arise from diffraction patterns like those appearing in figure 4(a). One immediately notes that the maxima which compose the calculated binary encounter peak do not appreciably change their position with varying ϑ^L. Instead their relative intensities are strongly angle dependent. The calculations show nicely how the binary encounter strength shifts from one maximum to the next, and how a splitting is introduced whenever two neighbouring maxima share comparable amounts of BE strength. The angular position at which a splitting occurs coincides approximately with the position of a diffraction minimum in the corresponding elastic scattering cross section of figure 4(a). The calculations predict the shift from the maximum of highest energy, located at 1200 eV, to the next maximum at 800 eV to take place at angles around 15° to 16° in the I^{7+} case, and at angles around 22° in the I^{23+} case, in very good agreement with the experimental results.

In the I^{7+} case a second splitting is expected to occur at angles between 40° and 45°. As seen in figure 3, no such splitting can be observed in the experimental results. At these larger angles, a contribution from projectile-electron loss still persists at 330 eV, along with the BE peak located around 750 eV. The BE peak loses intensity with increasing angle as predicted by the calculation, but the subsequent emergence of a BE peak at the lower energy of approximately 450 eV cannot be confirmed. While its position would roughly coincide with that of the electron loss peak, no increase in intensity is seen in this energy region between 35° and 50°.

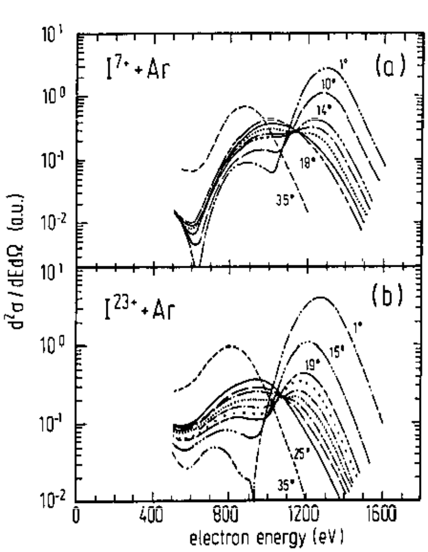

Figure 5. Calculated double differential model cross sections for the production of binary encounter electrons. In (a) the cross sections between 14° and 18° were calculated in steps of 1° to exhibit the transitional behaviour of the BE strength. The same remark applies for (b) between 19° and 25°.

From the calculated DDCS for I^{7+} and I^{23+} on Ar, single differential cross sections $d\sigma/d\Omega$ for the production of BE electrons were determined by integrating over the BE region and are shown in figure 4(*b*). These are compared to the experimental binary encounter electron yields, which were extracted from the data in the following way. The experimental DDCS contain a component which decreases exponentially with increasing energy and which underlies the binary encounter peak. The electrons which contribute to this exponential component originate from non-binary processes involving scattering in the two-centre potential of the combined projectile–target system. An exponential was therefore subtracted from the binary encounter peak, and the resulting net area taken as the binary electron yield. The experimental yield for I^{7+} was normalized to the calculated I^{7+} yield at 0°, and this same normalization was subsequently used for the I^{23+} yield. The experimental yield curves are also shown in figure 4(*b*).

While the experimental and calculated curves for I^{7+} are nearly identical at forward angles, the experimental I^{23+} yield drops faster with increasing angle than the calculated one. In both cases the experimental yields are, at large angles, much smaller than the calculated ones, making the observation of additional diffraction minima at larger angles more difficult. This latter point was demonstrated for the I^{7+} case for angles above 35° in figure 3, where the lack of BE strength precluded the observation of a second diffraction minimum. This experimentally observed early disappearance of the BE feature is presumably caused by a breakdown of the binary encounter approximation, which assumes the residual target to have a negligible influence on the scattering process. This condition is satisfied as long as the amount of energy transferred to the electron is sufficiently large, which is the case for small impact parameters and high projectile velocities. In the present work the projectile velocity is about 5 au, so only small impact parameters leading to small scattering angles will provide the necessary energy transfer. At larger scattering angles, corresponding to larger impact parameters, the influence of the target and projectile fields upon the electron may become comparable, so the electron will acquire a continuous energy distribution characteristic of a two-centre potential scattering.

4. Conclusions

The data presented here show that an 'anomalous' behaviour of the binary encounter electron peak is a phenomenon not confined to very heavy projectiles but is also observed in the collisions of not so heavy and not so strongly screened ions such as I^{23+}. Double differential binary encounter cross sections were calculated using model potentials for I^{7+} and I^{23+}. These screened potentials give rise to pronounced diffraction patterns in the elastic scattering cross section for target electrons, which in turn are responsible for either a splitting of the binary encounter peak or a sudden shift in its position. The calculations reproduce very well the basic features of the angular dependence of the binary encounter peak, i.e., the near constancy of the peak position over a large angular interval and the sudden intensity shift of the BE strength between discrete positions at a well defined angle, whose calculated value also agrees well with the observed one. The fact that these features are strongly projectile dependent, and that they can be connected quantitatively to the diffraction patterns appearing in the elastic scattering of free electrons from that projectile, suggests that binary encounter electrons could be used as a tool to probe the electronic charge distribution within a clothed ion.

Acknowledgments

We would like to acknowledge the assistance received from Dr R Repnow and staff members of the Emperor tandem accelerator of the MPI Heidelberg. Two of the authors gratefully acknowledge financial support during the course of the present investigation: JLS from the Fullbright Commission and the Alexander von Humboldt foundation for research fellowships and HEW from the Conselho Nacional de Desenvolvimento Cientifico e Tecnologico (Brazil) for a post-doctoral grant. Financial support by DFG and BMFT, and travel support by a NATO grant is gratefully acknowledged.

References

Bhalla C P and Shingal R 1991 *J. Phys. B: At. Mol. Opt. Phys.* **24** 3187

Drepper F and Briggs J S 1976 *J. Phys. B: At. Mol. Phys.* **9** 2063

Hagmann S, Wolff W, Shinpaugh J L, Wolf H E, Olson R E, Bhalla C P, Shingal R, Kelbch C, Herrmann R, Jagutzki O, Dörner R, Koch R, Euler J, Ramm U, Lencinas S, Dangendorf V, Unverzagt M, Mann R, Mokler P, Ullrich J and Schmidt-Böcking H 1992 *J. Phys. B: At. Mol. Opt. Phys.* **25** L287

Jagutzki O, Hagmann S, Schmidt-Böcking H, Olson R E, Schultz D R, Dörner R, Koch R, Skutlartz A, Gonzales A, Quinteros T B, Kelbch C and Richard P 1991 *J. Phys. B: At. Mol. Opt. Phys.* **24** 2579

Kelbch C 1991 *GSI-Report* GSI-91-12 April 1991

Kelbch C, Hagmann S, Kelbch S, Mann R, Olson R E, Schmidt S and Schmidt-Böcking H 1989 *Phys. Lett.* **139A** 304

Kelbch C, Koch R, Hagmann S, Ullmann K, Schmidt-Böcking H, Reinhold C O, Schultz D R, Olson R E and Kraft G 1992 *Z. Phys.* D **22** 713

Kessler J and Lindner H 1965 *Z. Phys.* **183** 1

Lee D H, Richard P, Zouros T J M, Sanders J M, Shinpaugh J L and Hidmi H 1990 *Phys. Rev.* A **41** 4816

Macek J 1970 *Phys. Rev.* A **1** 235

Olson R E, Reinhold C O and Schultz D R 1990 *J. Phys. B: At. Mol. Opt. Phys.* **23** L455

Reinhold C O, Schultz D R and Olson R E 1990 *J. Phys. B: At. Mol. Opt. Phys.* **23** L591

Reinhold C O, Schultz D R, Olson R E, Kelbch C, Koch R and Schmidt-Böcking H 1991 *Phys. Rev. Lett.* **66** 1842

Richard P, Lee D H, Zouros T J M, Sanders J M and Shinpaugh J L 1990 *J. Phys. B: At. Mol. Opt. Phys.* **23** L213

Salin A 1969 *J. Phys. B: At. Mol. Phys.* **2** 1225

Schultz D R and Olson R E 1991 *J. Phys. B: At. Mol. Opt. Phys.* **24** 3409

Shingal R, Chen Z, Karim K R, Lin C D and Bhalla C P 1990 *J. Phys. B: At. Mol. Opt. Phys.* **23** L637

Stolterfoht N, Schneider D, Burch D, Wiemann H and Risley S 1974 *Phys. Rev. Lett.* **33** 59

Wang J, Reinhold C O and Burgdörfer J 1991 *Phys. Rev.* A **44** 7243